International Journal of Nanomedicine

Dovepress

open access to scientific and medical research

Open Access Full Text Article

ORIGINAL RESEARCH

Photodynamic Therapy Using RGD-Functionalized Quantum Dots Elicit a Potent Immune Response in a Syngeneic Mouse Model of Pancreatic Cancer

Ming-Ming Li*, Yi Zhang*, Fang Sun, Man-Xiu Huai, Fei-Yu Zhang, Jia-Xing Pan, Chun-Ying Qu, Feng Shen, Zheng-Hong Li, Lei-Ming Xu

Department of Gastroenterology, Xinhua Hospital, School of Medicine, Shanghai Jiaotong University, Shanghai, People's Republic of China

*These authors contributed equally to this work

Correspondence: Lei-Ming Xu; Yi Zhang, Department of Gastroenterology, Xinhua Hospital, School of Medicine, Shanghai Jiaotong University, 1665 Kongjiang Road, Shanghai, People's Republic of China, 200092, Tel/Fax +86 21 2507 8999, Email xuleiming@xinhuamed.com.cn; zhangyi02@xinhuamed.com.cn

Purpose: Photodynamic therapy (PDT) induces anti-tumor immune responses by triggering immunogenic cell death in tumor cells. Previously, we demonstrated that novel QDs-RGD nanoparticles exhibited high efficiency as photosensitizers in the treatment of pancreatic cancer. However, the underlying mechanism of the anti-tumor immune effects induced by the photosensitizer remains unknown. This study assessed the anticancer immune effect of QDs-RGD, as well as the conventional photosensitizer chlorine derivative, YLG-1, for comparison, against pancreatic cancer in support of superior therapeutic efficacy.

Methods: The pancreatic cancer cell line, Panc02, was used for in vitro studies. C57BL/6 mice bearing pancreatic cancer cell-derived xenografts were generated for in vivo studies to assess the anti-tumor effects of QDs-RGD-PDT and YLG-1-PDT. The immunostimulatory ability of both photosensitizers was examined by measuring the expression of damage-associated molecular patterns (DAMP), such as calreticulin (CRT), assessing dendritic cell (DC) maturation, and analyzing cytokine expression. The specific immunity of QDs-RGD and YLG-1-PDT on distant tumor were determined by combining PDT with anti-CTLA-4 antibody.

Results: QDs-RGD-PDT and YLG-1-PDT significantly inhibited pancreatic cancer cell growth in a dose- and time-dependent manner. While both photosensitizers significantly promoted CRT release, DC maturation, and interferon γ (IFN-γ) and tumor necrosis factor α (TNF-α) expression, QDs-RGD exerted a stronger immunostimulatory effect than YLG-1. Combination treatment with QDs-RGD and CTLA-4 blockade was able to significantly inhibit the growth of distant tumors.

Conclusion: QDs-RGD is a novel and effective PDT strategy for treating pancreatic tumors by inducing anti-tumor immune responses.

Keywords: quantum dots, RGD peptides, cancer immunotherapy, pancreatic neoplasm

Introduction

Pancreatic cancer is among the most lethal malignancies worldwide, with a 5-year overall survival (OS) rate of ~10%.[1–3] Postoperative adjuvant chemotherapy (eg, modified FOLFIRINOX) can prolong the postoperative survival of pancreatic cancer patients, however, high-dose chemotherapy is associated with common and serious side effects.[4–7] Thus, there is an urgent need for the development of novel neoadjuvant therapies with high efficacy and specificity and low systemic toxicity.

In recent years, photodynamic therapy (PDT) has emerged as a new cancer treatment modality and attracted increasing attention from researchers.[8–10] Recently, we synthesized quantum dots conjugated with arginine-glycine-aspartic acid (QDs-RGD). QDs are nanocrystals consisting of elements belonging to group II–VI or group III–V with a 2–10 nm diameter. They have a large absorption spectrum, narrow emission bands, and a high molar extinction coefficient, suggesting that they can serve as potential photosensitizers in PDT.[11–13] Furthermore, the RGD peptide sequence is an integrin antagonist that can link to integrin αvβ3, playing a critical role in regulating tumor growth, metastasis, and angiogenesis.[14–16] Our previous studies

Received: 20 May 2024
Accepted: 5 September 2024
Published: 12 September 2024

demonstrated the potential applications of QDs-RGD as photosensitizers in the PDT of pancreatic cancer cells in vitro and in vivo, which exhibited high selectivity and efficiency against pancreatic cancer.[17–19] However, the phototherapeutic effects of these nanocrystals on pancreatic cancer and the underlying mechanisms for these effects remain unexplored.

Research has shown that reactive oxygen species (ROS) generated by PDT can drive immunogenic cell death (ICD) in tumor cells and boost antineoplastic immune responses.[8,20–22] Tumor cells undergoing ICD exhibit superior immunogenic potential through the expression and release of damage-associated molecular patterns (DAMP), including calreticulin (CRT), high-mobility group box 1 (HMGB1) protein, and adenosine triphosphate (ATP).[21,23–25] ICD stimulates multiple alterations in dying tumor cells, with CRT exposure serving as an "eat me" signal, HMGB1 efflux serving as a "danger" signal and ATP functioning as a "find me" signal, attracting and activating antigen-presenting cells and inducing an adaptive immune response.[26–28] An assessment of dendritic cell (DC) maturation using flow cytometry has illustrated how QDs-RGD-mediated PDT induces the immune response. DCs are one of the most important antigen-presenting cell types, playing an important role in both innate and adaptive immune processes.[29,30] Once exposed to antigens, immature DCs engulf and process antigens into peptides to exert immune response functions in adjacent lymph nodes.[31,32] The secretion of DC-specific cytokines, such as interferon γ (IFN-γ) and tumor necrosis factor α (TNF-α), is also an indicator of immune activation.[33,34]

In in vivo experiments, cytotoxic CTLA-4 blockade is shown to inhibit the immune-suppressive effect of regulatory T cells (Treg). Anti-CTLA-4 antibodies bind with high affinity to the CTLA-4 molecule, altering the composition of immune cells in the tumor microenvironment, ultimately enhancing the immune response against cancer.[35–41]

The current study investigated the effects of QDs-RGD-PDT on pancreatic cancer, including whether this involved eliciting an effective anti-tumor immune response in a highly metastatic tumor mouse model. Group administered with anti-CTLA-4 antibodies exhibited a significant enhancement in immunotherapy, and it did not cause any harmful effects to the mice themselves. The conventional photosensitizer chlorine derivative, (17R, 18R) −2- (1-hydroxyethyl) −2-divinyl chloride E6 trisodium salt (YLG-1), which is a dihydroporphyrin monomer derivative extracted from Spirulina platensis, was used as a comparison, for the reason that it previously exhibited high efficiency as photosensitizer in treatment of pancreatic cancer.[42,43] The findings illustrated that the synergistic photodynamic-immunologic effects of QDs-RGD-PDT could serve as a basis for future research on the mechanism of immune regulation.

Materials and Methods

Materials

QD705 consisting of cadmium selenide cores with a zinc sulfide shell and carboxylate-derivatized outer coating was purchased from Invitrogen (Carlsbad, CA, USA). Cyclic RGD peptide was obtained from GL Biochem (Shanghai, China). QD705 and RGD were conjugated to prepare QDs-RGD using the Qdot® Antibody Conjugation kit (Life Technologies, Carlsbad, CA, USA) according to the manufacturer's instructions. QDs705 and RGD were conjugated to prepare QDs-RGD according to the Qdot® Antibody Conjugation kit (Life Technologies, Carlsbad, CA, USA) manufacturer's instructions. The detailed operational steps were reported previously.[17,18]

The 650-nm laser PDT instrument was provided by Guilin Xingda Photoelectric Medical Equipment Co., Ltd (Guilin, China). YLG-1 was provided by Guilin Huiang Biochemistry Pharmaceutical Co., Ltd (Guilin, China), dissolved in phosphate buffer solution (PBS; Solarbio, China) to obtain a 10 mg/mL solution, and stored at 4 °C.

Characterization of QDs-RGD Particles

The optical absorption spectra of QDs-RGD nanoparticles were recorded using ultraviolet-visible (UV-Vis; UV-2550; Shimadzu, Kyoto, Japan) and fluorescence spectrophotometers (LS-55; PerkinElmer, Waltham, MA, USA). The size and morphology of nanoparticles were measured using transmission electron microscopy (H-600; Hitachi Tokyo, Japan).

Cell Culture

The murine pancreatic cancer cell line, Panc02, was purchased from the cell bank of the Type Culture Collection of the Chinese Academy of Sciences (Shanghai, China). Panc02 cells were cultivated in DMEM media (GIBCO, Life Technologies, USA) supplemented with 10% FBS (GIBCO), and 1% Penicillin-Streptomycin at 37°C and 5% CO_2.

In vitro PDT and Cell Counting Kit-8 Assay to Assess Cell Viability

Panc02 cells were inoculated on 96-well plates and incubated for 24 h before treatment. The cells were incubated with different concentrations of QDs-RGD (0–2.5 μmol/L) or YLG-1 (0–1 μg/mL) for 3 h at 37°C and then washed thoroughly with cell culture media to remove the unbound photosensitizers. The cells were then incubated with 2.0 μmol/L QDs-RGD or 0.5μg/mL YLG-1 without irradiation for different time periods. In a separate experiment, the cells were incubated with the indicated dose of QDs-RGD or YLG-1 for a specified time and irradiated at 5 to 30 J/cm^2 using ZF-20D Ultraviolet Analyzing Equipment at a wavelength of 365 nm and power of 20–60 mW/cm^2. The Cell Counting Kit-8 (CCK-8; Dojindo, Kumamoto, Japan) was used to assess cell viability. In brief, after the cells were incubated with QDs-RGD and light stimulation, 10 μL CCK-8 was added to each well of the 96-well plates, and the absorbance at 450 nm was recorded using a Thermo-max microplate reader (Thermo Fisher Scientific, Waltham, MA, USA).

Determination of Immunogenic Cell Death in vitro

Cells were seeded on 24-well plates at a density of 5×10^5 cells/well and cultured for 24 h. The cells were then incubated with 2.0 μmol/L QDs-RGD for 3 h and irradiated at 650 nm (20 J/cm^2). To detect surface CRT expression, the cells were incubated with anti-CRT primary antibody for 30 min and stained with Alexa 488-conjugated monoclonal secondary antibody for an additional 30 min in the dark. The cells were then analyzed by flow cytometry. To visualize surface CRT by immunofluorescent staining, the cells were inoculated onto 24-well plates with prepared slides under the same experimental conditions. The adherent cells were washed twice with PBS and fixed with 4% paraformaldehyde for 20 min. CRT staining was processed as described above. After staining with DAPI for 5 min, the cells were examined by confocal laser scanning microscopy (CLSM) (Leica, Germany).

DC Maturation

Bone marrow-derived monocytes were extracted from 6–8 weeks old C57BL/6 mice and cultured in complete RPMI containing mouse recombinant GM-CSF (20 ng/mL) and IL-4 (20 ng/mL) for 6 days to promote differentiation into CD11c+ BMDCs. The BMDCs were stimulated with treated tumor cells for 24 h and stained with fluorescence-labeled antibodies against CD11c, CD80, and CD86. CD80/CD86 double-positive DCs gated by CD11c+ were recognized as mature DCs.

Detection of Cytokines

Pro-inflammatory cytokines, including TNF-α (eBiosciences) and IFN-γ (eBiosciences), were measured in serum and DC medium supernatants using enzyme-linked immunosorbent assay (ELISA) kits following standard protocols.

Development of an in vivo Animal Model and Tumor-Specific Immunity

Female C57BL/6 mice (6–8 weeks) were purchased from the Shanghai Laboratory Animal Center of the Chinese Academy of Sciences. The Ethics Committee of Xinhua Hospital Affiliated to Shanghai Jiao Tong University School of Medicine approved the in vivo experiments. All experiments were conducted using the institutional protocols set by the China Association of Laboratory Animal Care. Panc02 cells (5×10^6) in 200 μL phosphate-buffered saline (PBS) were injected subcutaneously into the left backs of the mice. About 2 weeks after the tumor cell inoculation, when the tumors had reached a size of approximately 100 mm^3, 5 pmol QDs-RGD nanoparticles were injected into the tumors of each mouse. After 2 h, the mice were irradiated with a 650 nm laser at a power density of 100 mW/cm^2 for 30 min with a 1 min interval after every 2 min of light exposure.

To measure DC maturation in vivo, some of the mice in each group were sacrificed 3 days post-treatment. The lymph nodes were harvested, ground into a single cell suspension, and stained with anti-CD11c-FITC, anti-CD80-PE, and anti-CD86-PE-Cy7. Flow cytometry was used to detect the presence of mature DCs (CD11c+CD80+CD86+). To assess long-term tumor-specific immunity on distant tumor, 10 μg of anti-CTLA-4 antibody was intravenously injected into each mouse. Once the tumors had disappeared, the mice were rechallenged by injecting Panc02 tumor cells into their untreated flank. The tumor size of the mice was monitored daily. Tumor volume was calculated using the following formula: width^2 × length × 0.5.

Histopathology

The dissected organs of the mice in groups with anti-CTLA-4 antibody injection were fixed in 4% paraformaldehyde for 6 h, embedded in paraffin, and cut into 4 μm tissue sections. The slices were stained with hematoxylin-eosin (HE) and examined under a light microscope (Leica DMI4000 B; Leica Microsystems, Wetzlar, Germany).

Statistical Analysis

All experiments were replicated at least three times. Data are presented as the mean ± standard error of the mean (SEM). A two-tailed Student's *t*-test was used to test differences between two groups and a one or two-way ANOVA was used to test differences among multiple groups. All analyses were performed using GraphPad Prism 6.0. A p-value <0.05 was considered statistically significant.

Results

In vitro Phototoxicity Studies of QDs-RGD-PDT-Induced Pancreatic Cancer Cell Death

The PDT effect of QDs-RGD in vitro is shown in Figure 1. A representative transmission electron microscopy (TEM) image of QDs-RGD shows a spherical shape with a particle diameter of about 10 nm (Figure 1A). The novel nanoparticles dispersed well without agglomeration. The peaks of QDs-RGD in Figure 1B and C showed that the absorbance of QDs-RGD was the highest in the UV part of the spectrum, and decreased exponentially when approaching higher wavelengths. QDs-RGD had a luminescence emission peak at 700 nm. The CCK-8 assay was used to examine the viability of Panc02 cells in response to different QDs-RGD concentrations, incubation times, and light intensities to determine the most effective treatment regimen. To determine the best QDs-RGD concentration, the cells were treated with 0, 0.5, 1.0, 1.5, 2.0, or 2.5 μmol/L QDs-RGD for 3 h in the absence of light (Figure 1D). The results indicate that cell viability does not significantly decrease to a certain extent when the concentration of QDs-RGD increases. Obviously when the concentration of QDs-RGD reached above 2.0μmol/L, cell viability showed a greater reduction. It meant when

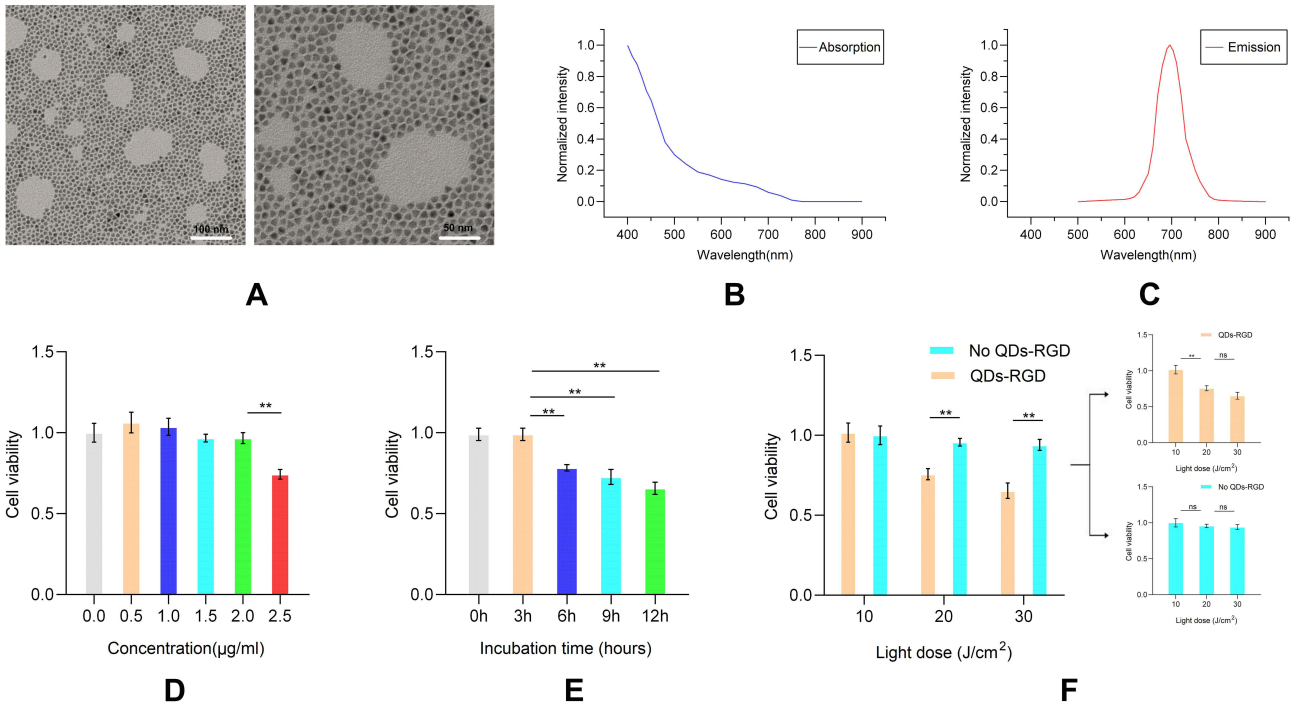

Figure 1 In vitro phototoxicity studies of QDs-RGD-PDT-induced pancreatic cancer cell death.
Notes: (**A**) TEM images of QDs-RGD, scale bar: left, 100nm; right 50nm; (**B**) Absorption spectra of QDs-RGD; (**C**) Fluorescence emission spectra of QDs-RGD; (**D**–**F**) Cell apoptosis assay of different concentration (**D**), incubation time (**E**) and light dose (**F**) measured by CCK-8. Data are expressed as means ± SEM (n = 3). $^{**}P < 0.01$, ns, not significant.
Abbreviations: QDs-RGD, quantum dots conjugated with arginine-glycine-aspartic acid peptide sequence; PDT, photodynamic therapy; TEM, transmission electron microscopy; CCK-8, cell counting kit-8; SEM, standard error of the mean.

the concentration of QDs-RGD reached or even exceeded a certain concentration, the toxicity of QDs-RGD would directly damage and influence Panc02 cells, which might cause the increased insecurity and uncertainty. To define the best incubation time, the cells were incubated with 2.0 μmol/L QDs-RGD for 0, 3, 6, 9 or 12 h without illumination. Longer incubation times were associated with lower viability (Figure 1E). Thus, 3 hours would be the best incubation time for the less reduction of cell viability of Panc02 cells. To assess the impact of light, the Panc02 cells were incubated with 2.0 μmol/L QDs-RGD for 3 h and illuminated with different light doses (0, 10, 20, or 30 J/cm^2). The illumination procedure was conducted by the ZF-20D Ultraviolet Analyzing Equipment at a wavelength of 365 nm and power of 20–60 mW/cm^2. More cell damage was observed at higher light doses. Illumination alone (10, 20, and 30 J/cm^2) without QDs-RGD had a limited impact on the Panc02 cells (Figure 1F), suggesting that QDs-RGD with illumination induced more cytotoxicity than illumination alone. Thus, 2.0 μmol/L QD-RGD at a light intensity of 20 J/cm^2 was used in subsequent in vitro experiments. It can generate effective PDT treatment without excessively affecting cell viability due to the toxicity of quantum dots themselves, which is a suitable prerequisite for subsequent ICD induction experiments.

The effect of QDs-RGD was next compared with that of the conventional photosensitizer chlorine derivative, YLG-1. The chemical structure, absorption and fluorescence emission spectra of YLG-1 is shown in Figure 2A–C. The same methods were used to determine the best experimental conditions of YLG-1-PDT in vitro (Figure 2D–F). Based on the results, 0.5 μg/mL YLG-1 at a light intensity of 10 J/cm^2 was used for subsequent experiments.

ICD Induction of QDs-RGD-PDT in vitro

After determining the best experimental conditions for QDs-RGD or YLG-1 treatment, the intracellular behavior and immune-activating effect of Panc02 cells were evaluated after PDT treatment in vitro. CRT exposure was used to verify the ICD of Panc02 cells. PDT-triggered ROS can induce the ICD of tumor cells that are under oxidative stress and activate the adaptive antitumor immune response. Higher expression of CRT on Panc02 cells can serve as an important

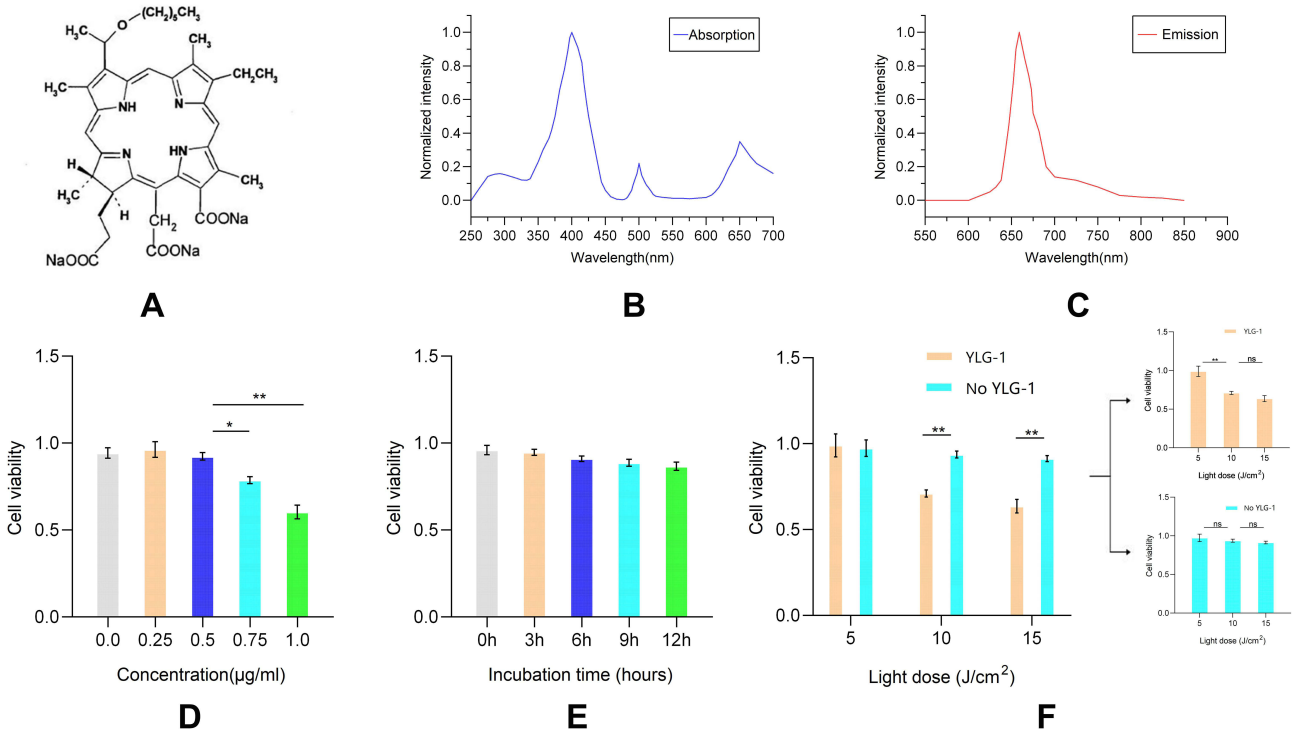

Figure 2 In vitro phototoxicity studies of YLG-1-PDT-induced pancreatic cancer cell death.
Notes: (**A**) Chemical structure of YLG-1; (**B**) Absorption spectra of YLG-1; (**C**) Fluorescence emission spectra of YLG-1; (**D–F**) Cell apoptosis assay of different concentration (**D**), incubation time (**E**) and light dose (**F**) measured by CCK-8. Data are expressed as means ± SEM (n = 3). *P < 0.05, **P < 0.01, ns, not significant.
Abbreviations: YLG-1, (17R,18R)-2-(1-hexyloxyethyl)-2-devinyl chlorine E6 trisodium salt; PDT, photodynamic therapy; CCK-8, cell counting kit-8; SEM, standard error of the mean.

indicator of ICD in vitro. Confocal laser scanning microscopy (CLSM) images demonstrated elevated CRT expression on the surface of Panc02 cells following 650 nm laser irradiation (Figure 3A). CRT exposing cell population was 5.2 and 4.1-fold higher in the QDs-RGD + Laser and YLG-1 + Laser treated groups in the PBS group, respectively, as shown by flow cytometry (Figure 3B and C).

The enhanced immunogenicity of pancreatic cancer cells can be used to potentiate DC maturation. Bone marrow (BM) cells were extracted from C57BL/6J mice, differentiated into BMDC, and coincubated with Panc02 cells for 24 h. The proportion of mature DCs (CD11c, CD80, and CD86 positive cells) was determined using flow cytometry. The PDT-treated QDs-RGD and YLG-1 groups induced 3.3- and 2.8-fold higher DC maturation than the PBS group, respectively, suggesting that these cells could elicit antitumor immunity by presenting tumor-specific antigens to T cells (Figure 4A and B). Consistent with the prior DC maturation results, significantly higher IFN-γ and TNF-α production was observed using QDs-RGD and YLG-1 treatment with illumination (Figure 4C), demonstrating that photosensitizers can enhance the immune response. These findings indicated that PDT treatment effectively enhanced the immune response and induced DC maturation. While both QDs-RGD and YLG-1 significantly promoted in vitro DC maturation, QDs-RGD promoted higher ICD than YLG-1.

Anti-Tumor Performance and Immunity Induced by QDs-RGD-Mediated PDT in vivo

After the Panc02 tumors grown on C57BL/6J mice had reached ~100 mm^3, the photosensitizers (5 pmol QDs-RGD or 5 mg YLG-1) were injected intratumorally. After 2 h, the mice were exposed to 650 nm light at a power density of 100 mW/cm^2. The tumor area was treated with irradiation twice on days 4 and 7. Tumor growth in different groups was measured using a caliper every 3 days (Figure 5A). Both the QDs-RGD and YLG-1-mediated PDT efficiently suppressed

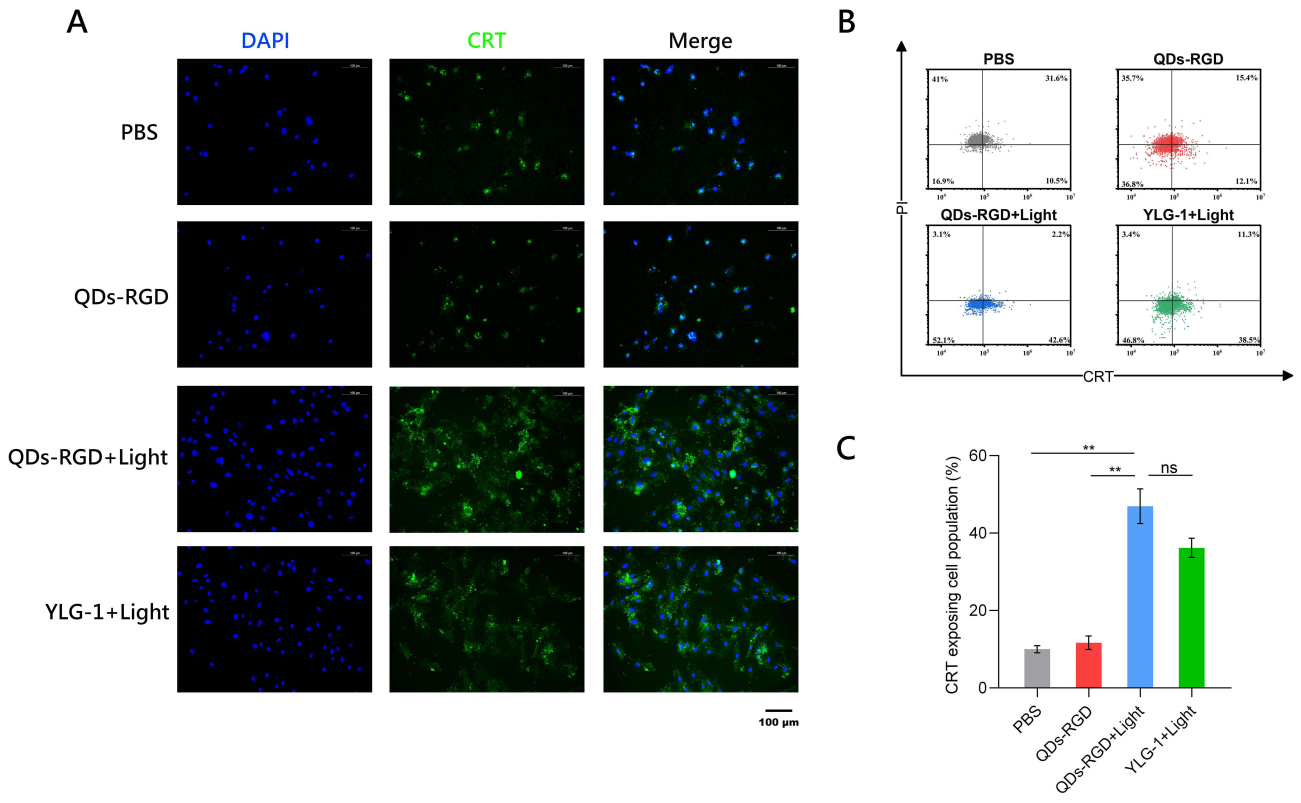

Figure 3 Expression of CRT on pancreatic cancer cell in vitro.

Notes: (**A**) CLSM image of the groups with different treatments. Blue, DAPI for nucleic acid staining. Green, CRT as specific marker of DAMP. Scale bars: 100 μm. (**B**) The flow cytometric analysis of PDT-induced CRT exposure of pancreatic cancer cells. (**C**) CRT exposing cell population of different groups measured by flow cytometry. Data are expressed as means ± SEM (n = 3). $^{**}P < 0.01$, ns, not significant.

Abbreviations: QDs-RGD, quantum dots conjugated with arginine-glycine-aspartic acid peptide sequence; YLG-1, (17R,18R)-2-(1-hexyloxyethyl)-2-devinyl chlorine E6 trisodium salt; PBS, phosphate-buffered saline; CLSM, confocal laser scanning microscopy; CRT, calreticulin; DAMP, damage-associated molecular pattern; SEM, standard error of the mean.

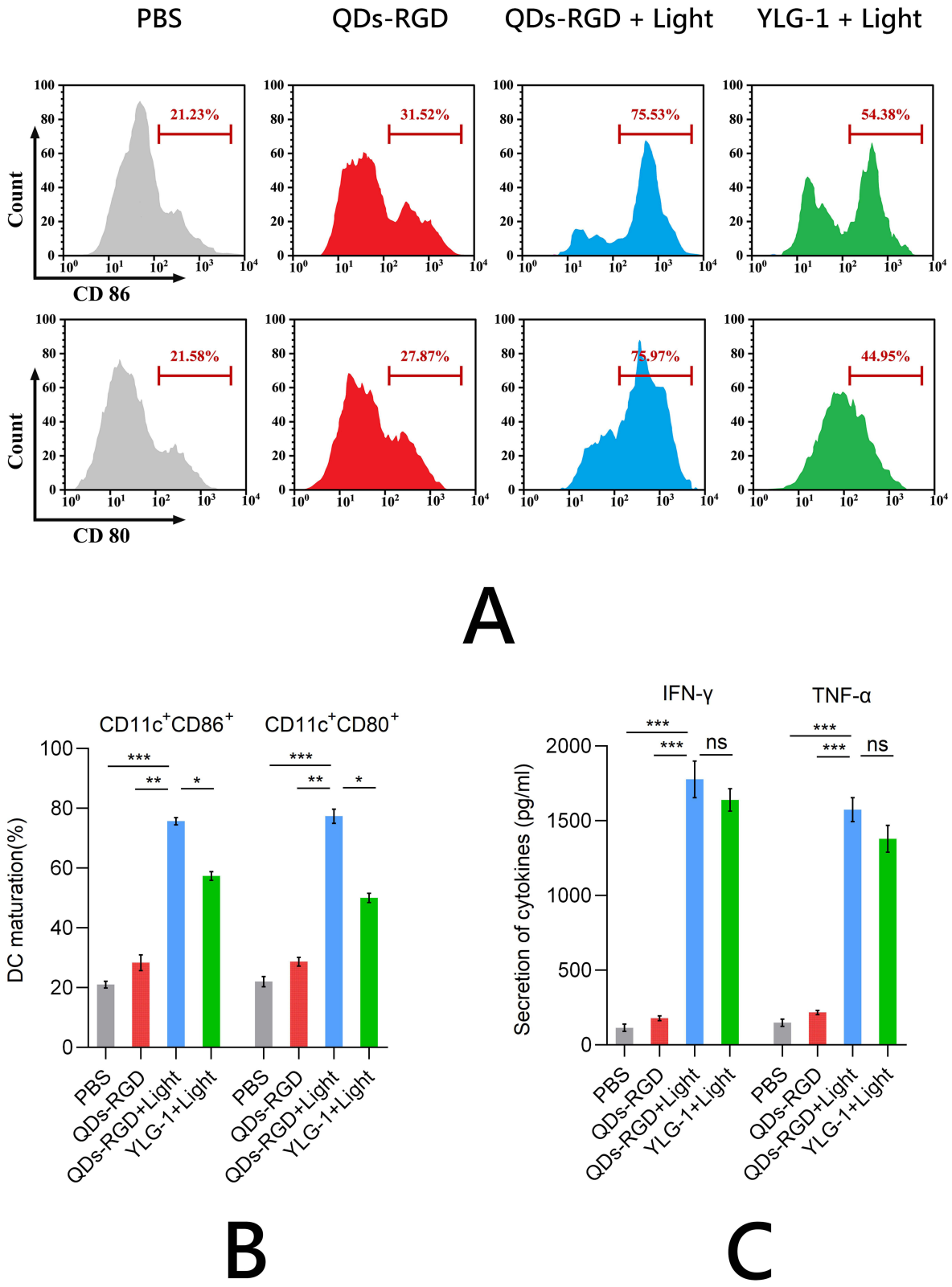

Figure 4 DC maturation and secretion of cytokines in vitro.

Notes: (**A**) and (**B**) Proportion of mature DCs (CD11c, CD80, and CD86 positive cells) determined using flow cytometry; (**C**) IFN-γ and TNF-α production measured by ELISA. Data are expressed as means ± SEM (n = 3). **P* < 0.05, ***P* < 0.01, ****P* < 0.001, ns, not significant.

Abbreviations: QDs-RGD, quantum dots conjugated with arginine-glycine-aspartic acid peptide sequence; YLG-1, (17R,18R)-2-(1-hexyloxyethyl)-2-devinyl chlorine E6 trisodium salt; PBS, phosphate-buffered saline; DC, dendritic cell; ELISA, enzyme-linked immunosorbent assay; SEM, standard error of the mean.

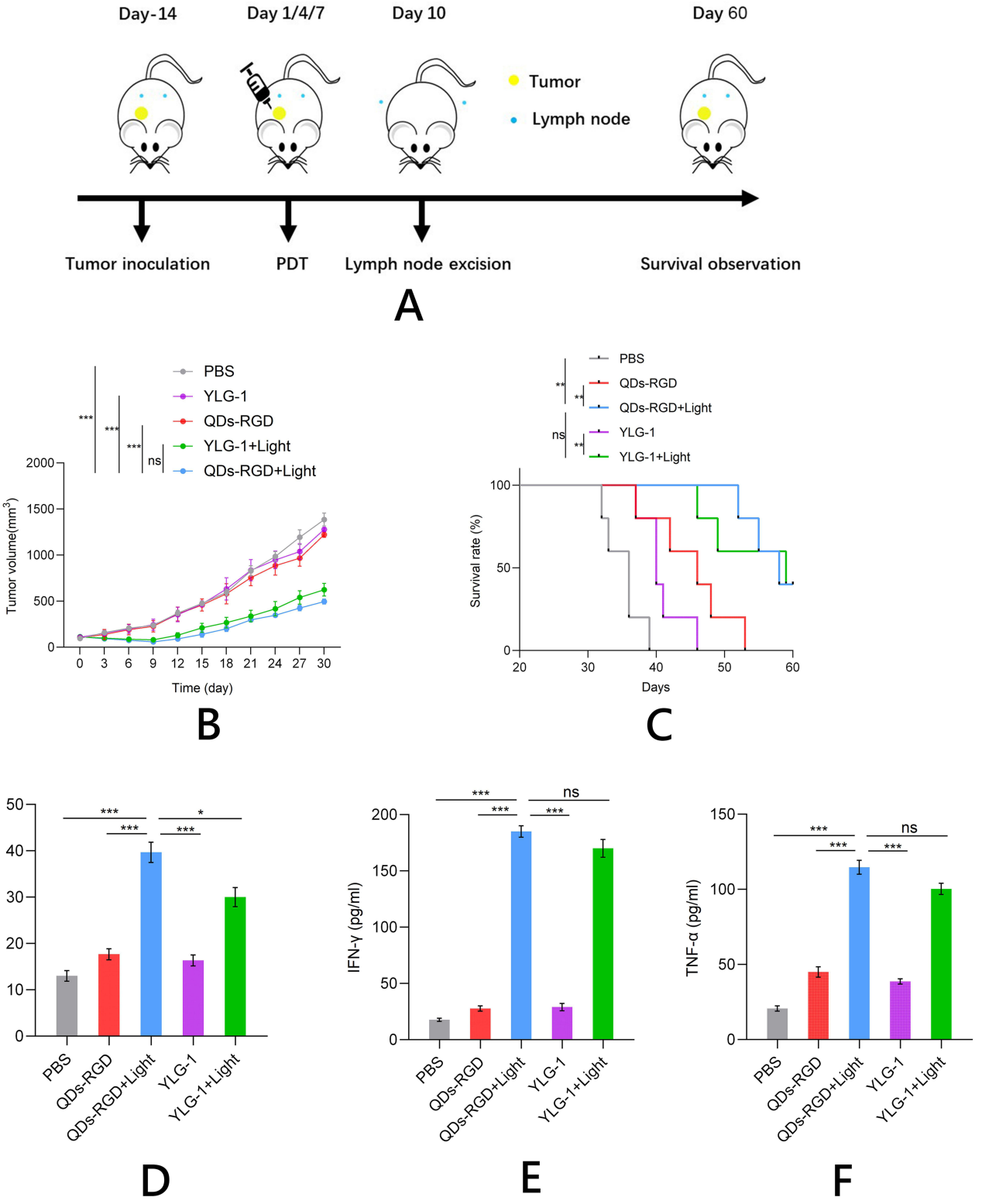

Figure 5 Anti-tumor performance and immunity induced by PDT in vivo.

Notes: (**A**) Schematic illustration of the experiment; (**B**) and (**C**) Growth curves for pancreatic tumors (**B**) and survival rate (**C**) on mice after various treatments indicated; (**D–F**) ICD induction of various treatments in vivo, including DC maturation (**D**), secretion of IFN-γ (**E**) and TNF-α (**F**). Data are expressed as means ± SEM (n = 5). *P < 0.05, **P < 0.01, ***P < 0.001, ns, not significant.

Abbreviations: QDs-RGD, quantum dots conjugated with arginine-glycine-aspartic acid peptide sequence; YLG-1, (17R,18R)-2-(1-hexyloxyethyl)-2-devinyl chlorine E6 trisodium salt; PBS, phosphate-buffered saline; PDT, photodynamic therapy; DC, dendritic cell; ICD, immunogenic cell death; SEM, standard error of the mean.

the tumors and prolonged the survival time of mice (Figure 5B and C). To further assess the anti-tumor immune effects, the mice were sacrificed 3 days after PDT and the draining lymph nodes were removed to measure the degree of DC maturation using flow cytometry (Figure 5D). QDs-RGD-based PDT promoted a relatively higher level of DC maturation than YLG-1 with light exposure or QDs-RGD and YLG-1 injection in the absence of light. IFN-γ and TNF-α production were also significantly upregulated in mice after QDs-RGD-PDT (Figure 5E and F), suggesting that cellular immunity was successfully induced by this treatment protocol.

Photoimmunotherapeutic Effect of QDs-RGD-PDT in Combination with CTLA-4 Checkpoint Blockade on Distant Tumors

We next assessed whether the robust immunological responses triggered by PDT with QDs-RGD could inhibit the growth of tumor cells that remained at distant sites after treatment. QDs-RGD-PDT was combined with CTLA-4 blockade therapy for in vivo cancer treatment. Panc02 tumor cells were subcutaneously inoculated into the left flanks of C57BL/6J mice. After 2 weeks, the tumors had reached ~100 mm^3 and the mice were divided into the following eight groups: (1) PBS, (2) anti-CTLA-4 antibody, (3) surgery alone, (4) surgery plus anti-CTLA-4 antibody, (5) QDs-RGD with irradiation, (6) QDs-RGD with irradiation plus anti-CTLA-4 antibody, (7) YLG-1 with irradiation, and (8) YLG-1 with irradiation plus anti-CTLA-4 antibody. QDs-RGD (5 pmol) was intratumorally injected into each tumor on the left flank of the mice in groups 5 and 6 and YLG-1 (5 mg) was intratumorally injected into the left flank of each mouse in groups 7 and 8. Two hours after the injection, the treated tumors in groups 5−8 were exposed to light exposure as described previously. The irradiation was repeated on days 1, 4, and 7. After irradiation (on days 2, 5, and 8), 10 μg anti-CTLA-4 (clone 9H10) antibody was intravenously injected into the mice in groups 2, 4, 6 and 8 (Figure 6A). The antibody dose was lower than that used in previous studies of checkpoint blockade therapy to avoid the inhibitory effect of this treatment. At day 9, after three times of irradiation and anti-CTLA-4 antibody treatment, Panc02 tumor cells were subcutaneously inoculated into the right flanks of the C57BL/6J mice for long-term observation, which were designed without direct treatment as an artificial model of abscopal tumors.

While QDs-RGD-PDT induced a strong immune response and partially delayed distant tumor growth, the tumor sizes were not significantly different from those in the PBS complete control group. After the combined use of CTLA-4 blockers, the combination therapy based on QDs-RGD-PDT and CTLA-4 blockers can significantly inhibit the growth of distant tumors (Figures 6B, C, S1 and S2). Furthermore, the growth of distant tumors was more significantly inhibited by combination therapy with QDs-RGD-PDT and CTLA-4 blockers than with YLG-1-PDT and CTLA-4 blockers. Survival analysis disclosed that the combination therapy of PDT and CTLA-4 blockade significantly prolonged the mice survival time when compared with other control groups (Figures 6D and S3–S5). These findings indicated that the novel QDs-RGD nanoparticles may serve as an effective adjuvant to boost anti-tumor immunity. QDs-RGD-PDT combined with CTLA-4 blockade may offer a strong synergistic anti-tumor immunological effect that effectively suppresses the growth of tumor cells, even for those without direct PDT.

All mice that received CTLA-4 antibodies (groups 2, 4, 6, and 8) were sacrificed to assess the effect of PDT, surgery, and especially, the CTLA-4 blockade on major organs, including the heart, lung, liver, kidney and spleen. Histological analysis indicated no signs of cell necrosis or organ damage, demonstrating that the treatments had a strong safety profile (Figure 7). Furthermore, the biochemical indicators of mice showed that the main indexes of groups combined with CTLA-4 blockage had no obvious changes compared with the PBS group. All values of each group were still in the reference range (Table 1), suggesting that there was limited systemic toxicity after the CTLA-4 blockage treatment.

Discussion

Our prior studies found that QDs-RGD-PDT exerts a significantly efficient photodynamic effect on tumor cells and may serve as a novel photosensitizer for the treatment of pancreatic cancer.[17–19] However, the mechanisms involved have remained unclear. In addition to its direct cytotoxic effects, PDT-mediated immunotherapeutic effects resulting from changes in the immune microenvironment were thought to play an important role.[44,45] The current study investigated the potential immunotherapeutic effects of QDs-RGD and assessed the possible mechanisms.

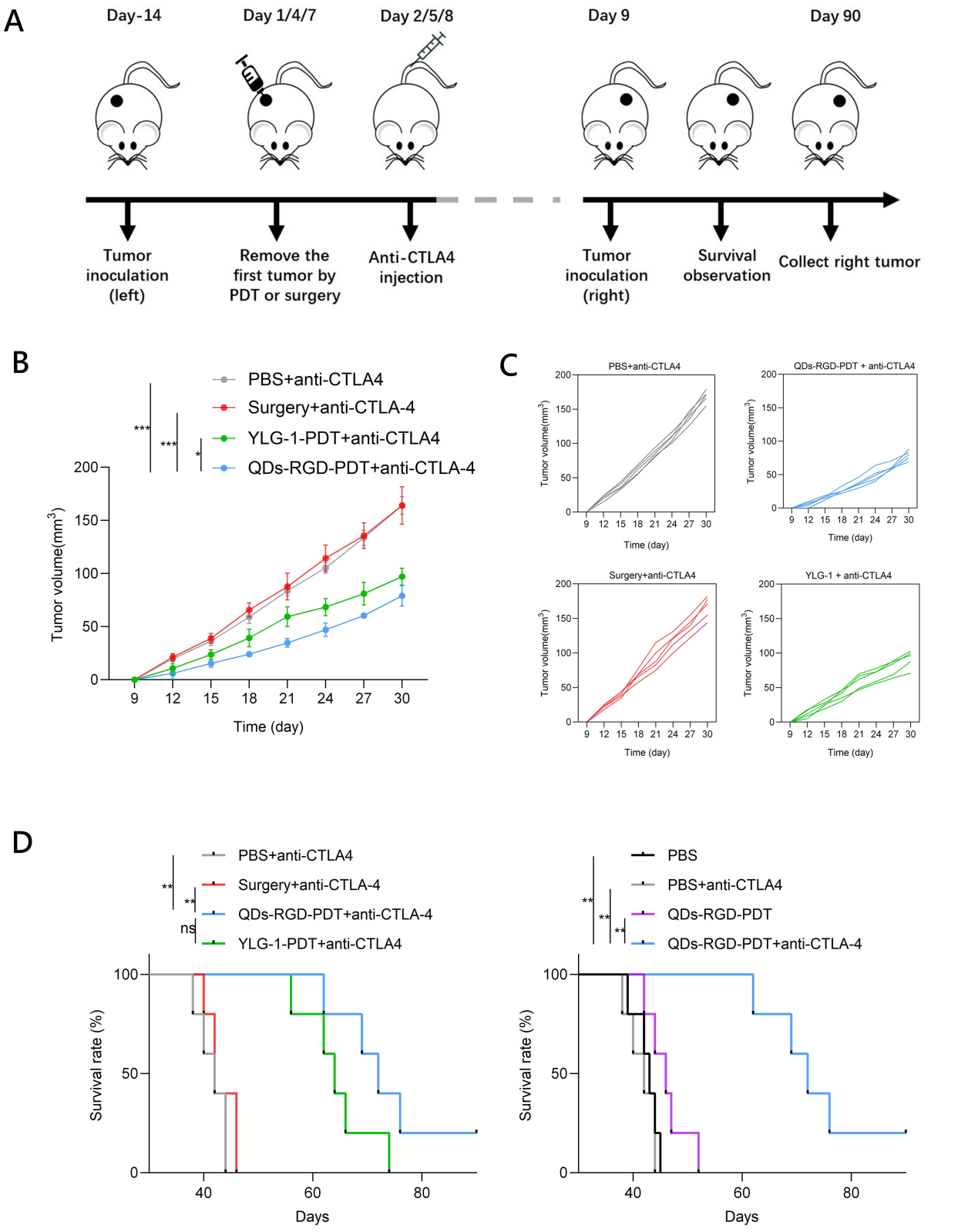

Figure 6 Photoimmunotherapeutic effect of PDT on distant tumors.

Notes: (**A**) Schematic illustration of the experiment; (**B**) Growth curves for the distant tumors on mice after various treatments indicated (n = 5 per group); (**C**) Individual tumor growth curves during the treatment; (**D**) Survival rate on mice after various treatments indicated. Data are expressed as means ± SEM (n = 5). **P* < 0.05, ***P* < 0.01, ****P* < 0.001, ns, not significant.

Abbreviations: QDs-RGD, quantum dots conjugated with arginine-glycine-aspartic acid peptide sequence; YLG-1, (17R,18R)-2-(1-hexyloxyethyl)-2-devinyl chlorine E6 trisodium salt; PBS, phosphate-buffered saline; PDT, photodynamic therapy; SEM, standard error of the mean; CTLA-4, cytotoxic T lymphocyte-associated antigen-4.

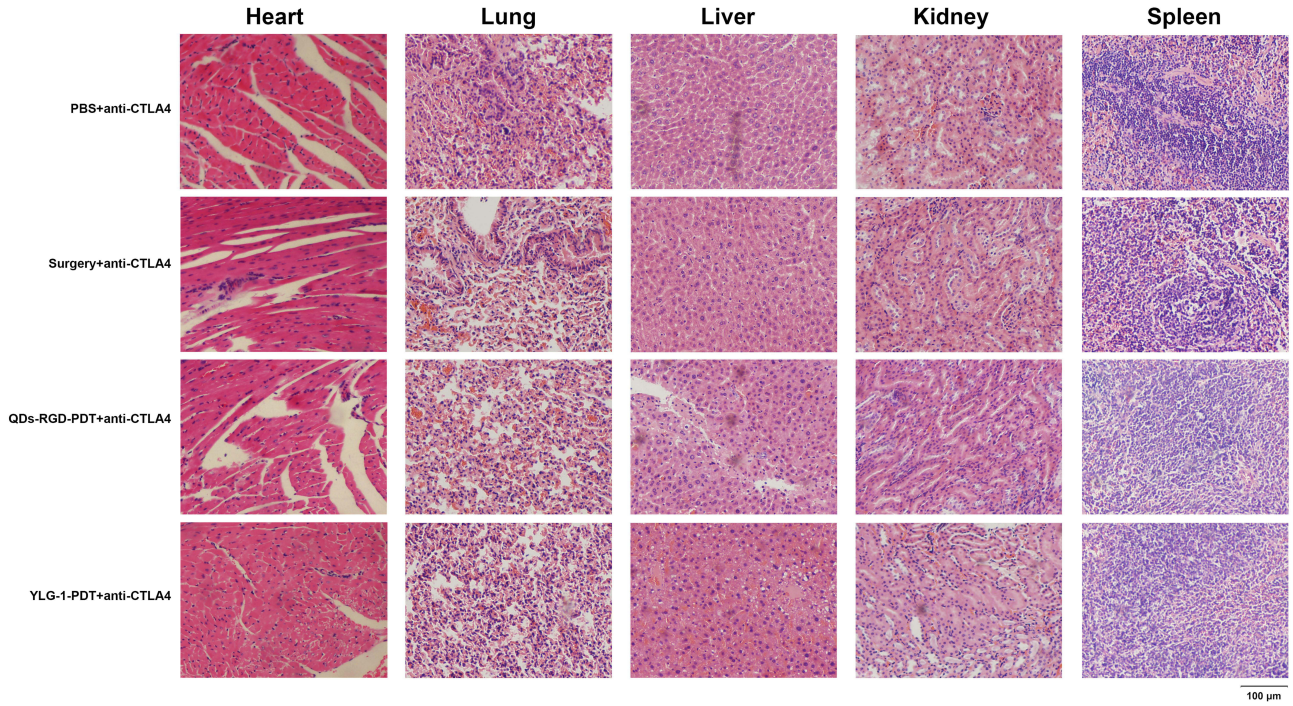

Figure 7 HE staining micrograph of organs from sacrificed mice in combination with CTLA-4 checkpoint blockade.
Notes: HE micrograph of tumor slices from four groups that received CTLA-4 antibodies. No signs of cell necrosis or organ damage were indicated in major organs, including the heart, lung, liver, kidney and spleen. Scale bar: 100μm.
Abbreviations: HE, hematoxylin and eosin; QDs-RGD, quantum dots conjugated with arginine-glycine-aspartic acid peptide sequence; YLG-1, (17R,18R)-2-(1-hexyloxyethyl)-2-devinyl chlorine E6 trisodium salt; PBS, phosphate-buffered saline; PDT, photodynamic therapy; CTLA-4, cytotoxic T lymphocyte-associated antigen-4.

It should be emphasized that the human pancreatic cancer cell line, SW1990 cells were mainly used in previous experiments.[17–19,42,43] Sometimes, we also used other human pancreatic cancer cells, such as Panc01, MIAPaCa-2, etc. We designed detailed experiments to explore and study the distribution and toxicity of quantum dots, the effectiveness of PDT treatment, and even the invasiveness of surviving cells after QDs-RGD-PDT. This time, we chose the mouse-derived pancreatic cancer cell line Panc02 to avoid the potential rejection by the mouse immune system. This approach could benefit the simulation of the immune microenvironment and aid in exploring the QDs-RGD-PDT mediated immunotherapy.

The photosensitizer QDs-RGD was synthesized by our research group according to the synthesis protocol included in the instruction manual. While QDs, a semiconductor nanomaterial, are relatively easy to prepare and have minimal cell toxicity under non-illuminated conditions, they can induce varying degrees of cell damage when exposed to light.[46–48] The RGD peptide sequence can bind to the integrin αvβ3 adhesion molecule, which is highly expressed on tumor cells but not easily detected in most normal organ systems, allowing QDs-RGD to successfully track tumor cells in vivo.[15,49]

Table 1 Some Biochemical Indicators of Mice at the End of Various Treatments

	ALP	ALT	UREA	CREA
PBS	88.3±18.5	41.6±5.9	7.4±0.7	32±6.4
PBS+anti-CTLA4	97±26.6	46.5±7.3	7.9±0.8	28±8.1
Surgery+ anti-CTLA4	82±19.5	50.1±9.7	8.2±1.1	43±8.8
QDs-RGD-PDT+ anti-CTLA4	122±30.7	55.6±8.7	9.1±0.8	36±10.4
YLG-1-PDT+ anti-CTLA4	112±25.8	59.8±7.6	8.5±0.8	27±6.6
Reference range	60–210(U/L)	30–135(U/L)	6.5–10.5(mmol/L)	20–75(μmol/L)

Abbreviations: ALP, alkaline phosphatase; ALT, alanine aminotransferase; UREA, blood urea; CREA, serum creatinine, PBS, phosphate-buffered saline, CTLA-4, cytotoxic T lymphocyte-associated antigen-4, QDs-RGD, quantum dots conjugated with arginine-glycine-aspartic acid peptide sequence, YLG-1, (17R,18R)-2-(1-hexyloxyethyl)-2-devinyl chlorine E6 trisodium salt, PDT, photodynamic therapy.

As a result, QDs-RGD has been increasingly used for cellular molecular tracking, in vivo tumor imaging, drug monitoring, and photodynamic therapy (PDT).[17,18,50]

Compared to traditional photosensitizers like verteporfin,[51] quantum dots require higher light doses to achieve effective cytotoxicity. However, the advantage of quantum dots is their ability to produce excellent excitation in the low-frequency range of the spectrum, and only low-frequency spectra can penetrate tissues effectively.[52–54] Despite the benefits of precise and effective treatment, the application of PDT is limited to surface lesions due to the insufficient penetration of light into biological tissues, preventing clinical treatment for deep abdominal tumors, particularly pancreatic tumors. These properties ensured the novel nanomaterial QDs-RGD could achieve better PDT effects in in vivo experiments.

Prior to initiating the in vitro experiments, we assessed the potential toxicity of the QDs and the cell necrosis caused by illumination. Nanomaterial-related toxicity is thought to result from the accumulation of heavy metal ions released from QD cores (such as Cd^{2+}).[55,56] Lower QD doses can minimize the toxic effects. Thus, before investigating the immunotherapeutic effects of QDs-RGD-PDT, three experiments were conducted to define the optimal conditions for QDs-RGD-PDT, including QD concentration, coincubation time, and light intensity. These served as the foundation for further investigation of the immunotherapeutic effects of PDT.

The optimal conditions were used for the in vitro QDs-RGD-PDT experiments. High levels of ROS generated during PDT treatment can accumulate in pancreatic cancer cells and may lead to the release of DAMPs, and induce ICD.[57–59] This process, in turn, can promote DC recognition and maturation and trigger an anti-tumor immune response. Thus, we assessed the immune expression of pancreatic cancer tumor cells after PDT. We specifically explored the increase in CRT externalization, which can serve as a "danger" signal, attracting and activating antigen-presenting cells and initiating the adaptive immune response. While the ICD effect was minimal in the control groups (including the blank and non-illuminated groups), CRT externalization was significantly increased in the PDT group. This finding confirmed our hypothesis from an in vitro perspective.

To further demonstrate the immunotherapeutic impact of PDT on pancreatic cancer growth in vivo, we exposed tumor-bearing mice to intratumoral irradiation. This method is widely accepted because it can achieve good therapeutic effects with lower doses of photosensitizer compared to traditional systemic administration methods such as tail vein injection.[60–62] Intratumoral injection is particularly suitable for tumors with poor blood supply, such as pancreatic cancer.[62–64] Willink[65] summarized a systematic review about the clinical trials of advanced pancreatic cancer patients using intratumoral injection method. The article pointed out that conventional administration methods like intravenous injection, could not accumulate well in tumors and yield unsatisfactory results, while intratumoral injection significantly improved the outcomes, potentially eliciting immunotherapy and prolonging the survival, making it a promising administration method. Although pancreatic cancer cells might have spread to surrounding tissues and the local treatment had limited effectiveness, it could effectively alleviate local pain and improve the quality of life, thus showing promise for future clinical applications. We would hypothesize that the photosensitizer can be directly injected into pancreatic cancer tissue using endoscopic ultrasound-guided fine-needle aspiration (EUS-FNA) and fiber optic insertion for illumination. This approach could increase the concentration of photosensitizer within a tumor and provide a sufficient light dose, enhancing the efficacy of PDT for pancreatic cancer.

After in vivo PDT treatment, tumor tissues, lymph nodes, and other samples were collected from all mouse groups, and immune-related tests were conducted. Mice treated with PDT showed significant tumor suppression and prolonged survival and significant changes in their immune response. This included a marked increase in DC maturation and higher IFN-γ and TNF-α serum expression. Importantly, QDs-RGD-PDT induced a significantly higher immunotherapeutic effect than YLG-1-PDT. This finding indicates that the novel QDs-RGD nanomaterial can more effectively activate the immune response in vivo, enhancing the immunotherapeutic effect and providing strong evidence for its clinical application. To further study the inhibitory effect of immunotherapy on pancreatic cancer, CTLA-4 checkpoint inhibitors were used in combination with PDT.

Cold cancers, characterized by low activity of suppressor immune cells, tend to respond less effectively to therapy compared to tumors categorized under hot immunity.[65–68] Cold immunity tumors include pancreatic cancer, colorectal cancer, prostate cancer, ovarian cancer, and breast cancer. In contrast, hot immune tumors, such as gastric cancer, lung cancer, cervical cancer, uterine cancer, melanoma, and bladder cancer, exhibit high levels of immune infiltration and are more responsive to immunotherapy. Pancreatic ductal adenocarcinoma (PDAC) is a malignant tumor characterized by

a highly fibrotic and immunosuppressive tumor microenvironment. This microenvironment, due to the presence of desmoplastic stroma, makes it difficult for immune cells to effectively infiltrate the tumor, thereby limiting the effectiveness of immunotherapy.[69–71] Anti-CTLA-4 antibodies bind with high affinity to the CTLA-4 molecule, altering the composition of immune cells in the tumor microenvironment. For example, increase the levels of CD80/CD86 on antigen-presenting cells (APCs), enhancing T cell activation; directly induce toxicity in regulatory T cells (Tregs); and promote the differentiation of CD4+ T cells into the Th1 subset, enhancing T cell infiltration into the tumor through the production of IFN-γ by these Th1 cells.[72–74] These are the potential mechanisms by which CTLA-4 blockade works, ultimately enhancing the immune response against cancer.

In our experiments, the group administered with anti-CTLA-4 antibodies exhibited a significant enhancement in immunotherapy, and it did not cause any harmful effects to the mice themselves. This compelling outcome underscores the potential of even a "cold" cancer like pancreatic cancer to elicit robust immune responses and ICD effects following PDT. The subsequent administration of anti-CTLA-4 antibodies further amplifies the therapeutic efficacy, indicating a synergistic relationship between PDT and immunotherapy. These findings provide valuable insights for the application of novel nanomaterials QDs-RGD in enhancing immunotherapeutic strategies.As QDs-RGD is still in the nascent stages of investigation, there remains a considerable period of exploration before its potential clinical applications can be realized. We have committed to continuing our research with a focus on refining the experimental design and filling the existing gaps in knowledge. Our team is dedicated to advancing the understanding of QDs-RGD and its immunotherapeutic effects, with the ultimate goal of facilitating its clinical implications.

Conclusion

In summary, QDs-RGD-mediated PDT has an immunomodulatory effect on the growth of pancreatic tumors. This treatment can significantly impact the survival of cancer cells by altering the immune microenvironment. Additional studies are needed to further investigate the mechanisms underlying these immunomodulatory effects to better inform the clinical application of QDs-RGD.

Abbreviations

BM, Bone marrow; CLSM, Confocal laser scanning microscopy; DAMP, Damage-associated molecular patterns; DC, dendritic cell; ELISA, Enzyme-linked immunosorbent assay; EUS-FNA, Endoscopic ultrasound-guided fine-needle aspiration; HE, Hematoxylin-eosin; ICD, Immunogenic cell death; OS, Overall survival; PBS, Phosphate buffer solution; PDT, Photodynamic therapy; QD, Quantum dots; RGD, Arginine-glycine-aspartic acid; ROS, Reactive oxygen species; SD, Standard deviation; TEM, Transmission electron microscopy; YLG-1, (17R, 18R) −2- (1-hydroxyethyl) −2-divinyl chloride E6 trisodium salt.

Acknowledgments

This study was supported by the National Natural Science Foundation of China (82003277 and 82172737) and Shanghai Municipal Education Commission (19411951605).

Author Contributions

All authors made a significant contribution to the work reported, whether that is in the conception, study design, execution, acquisition of data, analysis and interpretation, or in all these areas; took part in drafting, revising or critically reviewing the article; gave final approval of the version to be published; have agreed on the journal to which the article has been submitted; and agree to be accountable for all aspects of the work.

Disclosure

The authors report no conflicts of interest in this work.

References

1. Wood LD, Canto MI, Jaffee EM, Simeone DM. Pancreatic cancer: pathogenesis, screening, diagnosis, and treatment. *Gastroenterology*. 2022;163(2):386–402.e381. doi:10.1053/j.gastro.2022.03.056
2. Park W, Chawla A, O'Reilly EM. Pancreatic cancer: a review. *JAMA*. 2021;326(9):851–862. doi:10.1001/jama.2021.13027
3. Cai J, Chen H, Lu M, et al. Advances in the epidemiology of pancreatic cancer: trends, risk factors, screening, and prognosis. *Cancer Lett*. 2021;520:1–11. doi:10.1016/j.canlet.2021.06.027
4. Qin C, Yang G, Yang J, et al. Metabolism of pancreatic cancer: paving the way to better anticancer strategies. *Mol Cancer*. 2020;19(1):50. doi:10.1186/s12943-020-01169-7
5. Gugenheim J, Crovetto A, Petrucciani N. Neoadjuvant therapy for pancreatic cancer. *Updates Surg*. 2022;74(1):35–42. doi:10.1007/s13304-021-01186-1
6. Conroy T, Castan F, Lopez A, et al. Five-year outcomes of FOLFIRINOX vs gemcitabine as adjuvant therapy for pancreatic cancer: a randomized clinical trial. *JAMA Oncol*. 2022;8(11):1571–1578. doi:10.1001/jamaoncol.2022.3829
7. Zhang B, Zhou F, Hong J, et al. The role of FOLFIRINOX in metastatic pancreatic cancer: a meta-analysis. *World J Surg Oncol*. 2021;19(1):182. doi:10.1186/s12957-021-02291-6
8. Ji B, Wei M, Yang B. Recent advances in nanomedicines for photodynamic therapy (PDT)-driven cancer immunotherapy. *Theranostics*. 2022;12(1):434–458. doi:10.7150/thno.67300
9. Wang Y, Wang H, Zhou L, et al. Photodynamic therapy of pancreatic cancer: where have we come from and where are we going? *Photodiagn Photodyn Ther*. 2020;31:101876. doi:10.1016/j.pdpdt.2020.101876
10. Cramer GM, Cengel KA, Busch TM. Forging Forward in Photodynamic Therapy. *Cancer Res*. 2022;82(4):534–536. doi:10.1158/0008-5472.CAN-21-4122
11. Sobhanan J, Rival JV, Anas A, Sidharth Shibu E, Takano Y, Biju V. Luminescent quantum dots: synthesis, optical properties, bioimaging and toxicity. *Adv Drug Delivery Rev*. 2023;197:114830. doi:10.1016/j.addr.2023.114830
12. Tosat-Bitrián C, Palomo V. CdSe quantum dots evaluation in primary cellular models or tissues derived from patients. *Nanomedicine*. 2020;30:102299. doi:10.1016/j.nano.2020.102299
13. Widness JK, Enny DG, McFarlane-Connelly KS, Miedenbauer MT, Krauss TD, Weix DJ. CdS quantum dots as potent photoreductants for organic chemistry enabled by auger processes. *J Am Chem Soc*. 2022;144(27):12229–12246. doi:10.1021/jacs.2c03235
14. Kumar VB, Tiwari OS, Finkelstein-Zuta G, Rencus-Lazar S, Gazit E. Design of functional RGD peptide-based biomaterials for tissue engineering. *Pharmaceutics*. 2023;15(2):345. doi:10.3390/pharmaceutics15020345
15. Qian J, Zhou S, Lin P, et al. Recent advances in the tumor-penetrating peptide internalizing RGD for cancer treatment and diagnosis. *Drug Dev. Res.* 2023;84(4):654–670. doi:10.1002/ddr.22056
16. Ahmadi Z, Jha D, Kumar Gautam H, Kumar P, Kumar Sharma A. Cationic RGD peptidomimetic nanoconjugates as effective tumor targeting gene delivery vectors with antimicrobial potential. *Bioorg. Chem.* 2022;129:106197. doi:10.1016/j.bioorg.2022.106197
17. Li MM, Cao J, Yang JC, et al. Effects of arginine-glycine-aspartic acid peptide-conjugated quantum dots-induced photodynamic therapy on pancreatic carcinoma in vivo. *Int j Nanomed*. 2017;12:2769–2779. doi:10.2147/IJN.S130799
18. Li MM, Cao J, Yang JC, et al. Biodistribution and toxicity assessment of intratumorally injected arginine-glycine-aspartic acid peptide conjugated to CdSe/ZnS quantum dots in mice bearing pancreatic neoplasm. *Chem Biol Interact*. 2018;291:103–110. doi:10.1016/j.cbi.2018.06.014
19. He SJ, Cao J, Li YS, et al. CdSe/ZnS quantum dots induce photodynamic effects and cytotoxicity in pancreatic cancer cells. *World J Gastroenterol*. 2016;22(21):5012–5022. doi:10.3748/wjg.v22.i21.5012
20. Donohoe C, Senge MO, Arnaut LG, Gomes-da-Silva LC. Cell death in photodynamic therapy: from oxidative stress to anti-tumor immunity. *Biochim Biophys Acta Rev Cancer*. 2019;1872(2):188308. doi:10.1016/j.bbcan.2019.07.003
21. Alzeibak R, Mishchenko TA, Shilyagina NY, Balalaeva IV, Vedunova MV, Krysko DV. Targeting immunogenic cancer cell death by photodynamic therapy: past, present and future. *J Immuno Therap Can*. 2021;9(1):e001926. doi:10.1136/jitc-2020-001926
22. Nkune NW, Simelane NWN, Montaseri H, Abrahamse H. Photodynamic therapy-mediated immune responses in three-dimensional tumor models. *Int J Mol Sci*. 2021;22(23):12618. doi:10.3390/ijms222312618
23. Ullman NA, Burchard PR, Dunne RF, Linehan DC. Immunologic strategies in pancreatic cancer: making cold tumors hot. *J Clin Oncol*. 2022;40(24):2789–2805. doi:10.1200/JCO.21.02616
24. Li Z, Lai X, Fu S, et al. Immunogenic cell death activates the tumor immune microenvironment to boost the immunotherapy efficiency. *Advan Sci*. 2022;9(22):e2201734. doi:10.1002/advs.202201734
25. Hayashi K, Nikolos F, Lee YC, et al. Tipping the immunostimulatory and inhibitory DAMP balance to harness immunogenic cell death. *Nat Commun*. 2020;11(1):6299. doi:10.1038/s41467-020-19970-9
26. Ahmed A, Tait SWG. Targeting immunogenic cell death in cancer. *Mol Oncol*. 2020;14(12):2994–3006. doi:10.1002/1878-0261.12851
27. Jin F, Liu D, Xu X, Ji J, Du Y. Nanomaterials-based photodynamic therapy with combined treatment improves antitumor efficacy through boosting immunogenic cell death. *Int j Nanomed*. 2021;16:4693–4712. doi:10.2147/IJN.S314506
28. Li X, Zheng J, Chen S, Meng FD, Ning J, Sun SL. Oleandrin, a cardiac glycoside, induces immunogenic cell death via the PERK/elF2α/ATF4/CHOP pathway in breast cancer. *Cell Death Dis*. 2021;12(4):314. doi:10.1038/s41419-021-03605-y
29. Galati D, Zanotta S. Dendritic cell and cancer therapy. *Int J Mol Sci*. 2023;24(4). doi:10.3390/ijms24044253
30. Meng L, Teng Z, Yang S, et al. Biomimetic nanoparticles for DC vaccination: a versatile approach to boost cancer immunotherapy. *Nanoscale*. 2023;15(14):6432–6455. doi:10.1039/D2NR07071E
31. Wu L, Yan Z, Jiang Y, et al. Metabolic regulation of dendritic cell activation and immune function during inflammation. *Front Immunol*. 2023;14:1140749. doi:10.3389/fimmu.2023.1140749
32. Del Prete A, Salvi V, Soriani A, et al. Dendritic cell subsets in cancer immunity and tumor antigen sensing. *Cell Mol Immunol*. 2023;20(5):432–447.
33. Hilligan KL, Ronchese F. Antigen presentation by dendritic cells and their instruction of CD4+ T helper cell responses. *Cell Mol Immunol*. 2020;17(6):587–599.

34. Liu P, Kang C, Zhang J, et al. The role of dendritic cells in allergic diseases. *Int Immunopharmacol*. 2022;113(Pt B):109449. doi:10.1016/j.intimp.2022.109449
35. Hosseini A, Gharibi T, Marofi F, Babaloo Z, Baradaran B. CTLA-4: from mechanism to autoimmune therapy. *Int Immunopharmacol*. 2020;80:106221. doi:10.1016/j.intimp.2020.106221
36. De Silva P, Aiello M, Gu-Trantien C, Migliori E, Willard-Gallo K, Solinas C. Targeting CTLA-4 in cancer: is it the ideal companion for PD-1 blockade immunotherapy combinations? *Internat J Can*. 2021;149(1):31–41.
37. Coutzac C, Jouniaux JM, Paci A, et al. Systemic short chain fatty acids limit antitumor effect of CTLA-4 blockade in hosts with cancer. *Nat Commun*. 2020;11(1):2168. doi:10.1038/s41467-020-16079-x
38. Esmaily M, Masjedi A, Hallaj S, et al. Blockade of CTLA-4 increases anti-tumor response inducing potential of dendritic cell vaccine. *J Cont Rel*. 2020;326:63–74. doi:10.1016/j.jconrel.2020.06.017
39. Sharma P, Goswami S, Raychaudhuri D, et al. Immune checkpoint therapy-current perspectives and future directions. *Cell*. 2023;186(8):1652–1669. doi:10.1016/j.cell.2023.03.006
40. Williams KC, Gault A, Anderson AE, et al. Immune-related adverse events in checkpoint blockade: observations from human tissue and therapeutic considerations. *Front Immunol*. 2023;14:1122430. doi:10.3389/fimmu.2023.1122430
41. Safaeifard F, Goliaei B, Aref AR, et al. Distinct dynamics of migratory response to PD-1 and CTLA-4 blockade reveals new mechanistic insights for potential T-cell reinvigoration following immune checkpoint blockade. *Cells*. 2022;11(22):3534. doi:10.3390/cells11223534
42. Shen YJ, Cao J, Sun F, et al. Effect of photodynamic therapy with (17R,18R)-2-(1-hexyloxyethyl)-2-devinyl chlorine E6 trisodium salt on pancreatic cancer cells in vitro and in vivo. *World J Gastroenterol*. 2018;24(46):5246–5258. doi:10.3748/wjg.v24.i46.5246
43. Shen Y, Li M, Sun F, et al. Low-dose photodynamic therapy-induced increase in the metastatic potential of pancreatic tumor cells and its blockade by simvastatin. *J Photochem Photobiol B Biol*. 2020;207:111889. doi:10.1016/j.jphotobiol.2020.111889
44. Pan WL, Tan Y, Meng W, et al. Microenvironment-driven sequential ferroptosis, photodynamic therapy, and chemotherapy for targeted breast cancer therapy by a cancer-cell-membrane-coated nanoscale metal-organic framework. *Biomaterials*. 2022;283:121449. doi:10.1016/j.biomaterials.2022.121449
45. Zhang D, Xie Q, Liu Y, et al. Photosensitizer IR700DX-6T- and IR700DX-mbc94-mediated photodynamic therapy markedly elicits anticancer immune responses during treatment of pancreatic cancer. *Pharmacol Res*. 2021;172:105811. doi:10.1016/j.phrs.2021.105811
46. Chakraborty P, Das SS, Dey A, et al. Quantum dots: the cutting-edge nanotheranostics in brain cancer management. *J Cont Rel*. 2022;350:698–715. doi:10.1016/j.jconrel.2022.08.047
47. Zhu H, Ni N, Govindarajan S, Ding X, Leong DT. Phototherapy with layered materials derived quantum dots. *Nanoscale*. 2020;12(1):43–57. doi:10.1039/C9NR07886J
48. Fan J, Qian L. Quantum dot patterning by direct photolithography. *Nature Nanotechnol*. 2022;17(9):906–907. doi:10.1038/s41565-022-01187-0
49. Ma W, Wang X, Zhang D, Mu X. Research progress of disulfide bond based tumor microenvironment targeted drug delivery system. *Int j Nanomed*. 2024;19:7547–7566. doi:10.2147/IJN.S471734
50. Singh S, Raina D, Rishipathak D, et al. Quantum dots in the biomedical world: a smart advanced nanocarrier for multiple venues application. *Arch Pharm*. 2022;355(12):e2200299. doi:10.1002/ardp.202200299
51. Garg SJ, Hadziahmetovic M. Verteporfin photodynamic therapy for the treatment of chorioretinal conditions: a narrative review. *Clin Ophthalmol*. 2024;18:1701–1716. doi:10.2147/OPTH.S464371
52. Yang Q, Li F, Miao Y, et al. CdSe/ZnS quantum dots induced spermatogenesis dysfunction via autophagy activation. *J Hazard Mater*. 2020;398:122327. doi:10.1016/j.jhazmat.2020.122327
53. Abdellatif AAH, Younis MA, Alsharidah M, Al Rugaie O, Tawfeek HM. Biomedical applications of quantum dots: overview, challenges, and clinical potential. *Int j Nanomed*. 2022;17:1951–1970. doi:10.2147/IJN.S357980
54. Villalva MD, Agarwal V, Ulanova M, Sachdev PS, Braidy N. Quantum dots as a theranostic approach in Alzheimer's disease: a systematic review. *Nanomedicine*. 2021;16(18):1595–1611. doi:10.2217/nnm-2021-0104
55. Xu Q, Gao J, Wang S, Wang Y, Liu D, Wang J. Quantum dots in cell imaging and their safety issues. *J Mat Chem B*. 2021;9(29):5765–5779. doi:10.1039/D1TB00729G
56. Wei T, Zhang T, Tang M. An overview of quantum dots-induced immunotoxicity and the underlying mechanisms. *Environm Pollut*. 2022;311:119865. doi:10.1016/j.envpol.2022.119865
57. Fan JQ, Wang MF, Chen HL, Shang D, Das JK, Song J. Current advances and outlooks in immunotherapy for pancreatic ductal adenocarcinoma. *Mol Cancer*. 2020;19(1):32. doi:10.1186/s12943-020-01151-3
58. Sun F, Zhu Q, Li T, et al. Regulating glucose metabolism with prodrug nanoparticles for promoting photoimmunotherapy of pancreatic cancer. *Advan Sci*. 2021;8(4):2002746. doi:10.1002/advs.202002746
59. Jang Y, Kim H, Yoon S, et al. Exosome-based photoacoustic imaging guided photodynamic and immunotherapy for the treatment of pancreatic cancer. *J Cont Rel*. 2021;330:293–304. doi:10.1016/j.jconrel.2020.12.039
60. Yang Y, Wu M, Cao D, et al. ZBP1-MLKL necroptotic signaling potentiates radiation-induced antitumor immunity via intratumoral STING pathway activation. *Sci Adv*. 2021;7(41):eabf6290. doi:10.1126/sciadv.abf6290
61. Bian Z, Shi L, Kidder K, Zen K, Garnett-Benson C, Liu Y. Intratumoral SIRPα-deficient macrophages activate tumor antigen-specific cytotoxic T cells under radiotherapy. *Nat Commun*. 2021;12(1):3229. doi:10.1038/s41467-021-23442-z
62. Jiang Z, Zhang W, Zhang Z, Sha G, Wang D, Tang D. Intratumoral microbiota: a new force in diagnosing and treating pancreatic cancer. *Cancer Lett*. 2023;554:216031. doi:10.1016/j.canlet.2022.216031
63. Sun B, Bte Rahmat JN, Zhang Y. Advanced techniques for performing photodynamic therapy in deep-seated tissues. *Biomaterials*. 2022;291:121875. doi:10.1016/j.biomaterials.2022.121875
64. Tao J, Yang G, Zhou W, et al. Targeting hypoxic tumor microenvironment in pancreatic cancer. *J Hematol Oncol*. 2021;14(1):14.
65. Willink CY, Jenniskens SFM, Klaassen NJM, Stommel MWJ, Nijsen JFW. Intratumoral injection therapies for locally advanced pancreatic cancer: systematic review. *BJS Open*. 2023;7(3). doi:10.1093/bjsopen/zrad052
66. Majidpoor J, Mortezaee K. The efficacy of PD-1/PD-L1 blockade in cold cancers and future perspectives. *Clin Immunol*. 2021;226:108707. doi:10.1016/j.clim.2021.108707

67. Liu Y, Zheng P. Preserving the CTLA-4 checkpoint for safer and more effective cancer immunotherapy. *Trends Pharmacol Sci*. 2020;41(1):4–12. doi:10.1016/j.tips.2019.11.003
68. Liao L, Xu H, Zhao Y, Zheng X. Metabolic interventions combined with CTLA-4 and PD-1/PD-L1 blockade for the treatment of tumors: mechanisms and strategies. *Front Med*. 2023;17(5):805–822. doi:10.1007/s11684-023-1025-7
69. Chen H, Yang G, Xiao J, Zheng L, You L, Zhang T. Neoantigen-based immunotherapy in pancreatic ductal adenocarcinoma (PDAC). *Cancer Lett*. 2020;490:12–19. doi:10.1016/j.canlet.2020.06.011
70. Bockorny B, Grossman JE, Hidalgo M. Facts and Hopes in Immunotherapy of Pancreatic Cancer. *Clin Can Res*. 2022;28(21):4606–4617. doi:10.1158/1078-0432.CCR-21-3452
71. Panchal K, Sahoo RK, Gupta U, Chaurasiya A. Role of targeted immunotherapy for pancreatic ductal adenocarcinoma (PDAC) treatment: an overview. *Int Immunopharmacol*. 2021;95:107508. doi:10.1016/j.intimp.2021.107508
72. Zappasodi R, Serganova I, Cohen IJ, et al. CTLA-4 blockade drives loss of T(reg) stability in glycolysis-low tumours. *Nature*. 2021;591 (7851):652–658. doi:10.1038/s41586-021-03326-4
73. Zhou Y, Medik YB, Patel B, et al. Intestinal toxicity to CTLA-4 blockade driven by IL-6 and myeloid infiltration. *J Exp Med*. 2023;220(2). doi:10.1084/jem.20221333
74. Luoma AM, Suo S, Williams HL, et al. Molecular pathways of colon inflammation induced by cancer immunotherapy. *Cell*. 2020;182(3):655–671. e622. doi:10.1016/j.cell.2020.06.001